

A Semicontinuum Model for $\text{Si}_x\text{Ge}_{1-x}$ Alloys: Calculation of Their Elastic Characteristics and the Strain Field at the Free Surface of a Semi-Infinite Alloy

V.K. Tewary¹ and M. D. Vaudin²

Abstract: A semicontinuum Green's-function-based model is proposed for analysis of averaged mechanical characteristics of $\text{Si}_x\text{Ge}_{1-x}$. The atomistic forces in the model are distributed at discrete lattice sites, but the Green's function is approximated by the continuum GF in the far field and by the averaged lattice GF in the near field. Averaging is achieved by replacing Si and Ge atoms by identical hypothetical atoms that are x fraction Si and (1-x) fraction Ge. The parameters of the model are derived using the atomistic model from the interatomic potential between the hypothetical atoms. The interatomic potential is obtained from the radial embedded atom model proposed in an earlier paper. The parameters of the model potential are estimated partly by interpolation and partly by fitting the calculated and measured values of the cohesive energy and the lattice constant of $\text{Si}_x\text{Ge}_{1-x}$ as functions of x. The model is applied to calculate the elastic constants of $\text{Si}_x\text{Ge}_{1-x}$ and the displacement and the strain field at the free surface of a semi-infinite alloy for different values of x due to a buried point defect. The elastic constants predicted by the model are used to calculate the curvature of a single crystal of Si with a 49 nm epitaxial film of $\text{Si}(0.846)\text{Ge}(0.154)$. The calculated value (312.8 m) of the radius of curvature is in excellent agreement with the recently measured value (314.5 m) at our laboratory.

Keywords: Curvature of plates, elastic constants, interatomic potential, Mindlin problem, phonon Green's function, SiGe alloys, semi-continuum Green's function.

1 Introduction

We present a semicontinuum model of $\text{Si}_x\text{Ge}_{1-x}$ that accounts for the discrete lattice structure of the solid and relates it to the corresponding continuum model. The

¹ Materials Reliability Division, National Institute of Standards & Technology (NIST), Boulder, CO 80305, USA

² Ceramics Division, National Institute of Standards & Technology (NIST), Gaithersburg, MD 20899, USA

main application of this model is intended for the analysis of averaged thermal and mechanical characteristics of the solid. Examples of such characteristics are elastic strains, mechanical stability, and thermodynamic functions of the solid such as thermal conductivity and the specific heat.

$\text{Si}_x\text{Ge}_{1-x}$ refers to an alloy of Si and Ge, where x is the relative concentration of Si ($0 \leq x \leq 1$). This is a material of strong topical interest due to its crucial role in the modern nanoscale CMOS technology. The alloy $\text{Si}_x\text{Ge}_{1-x}$ is used for stretching the Si lattice, which results into enhanced carrier mobility and a significant increase in the efficiency of the devices. This has resulted in fabrication of sub 45 nm transistors with the possibility of even further reduction in the device dimensions. For excellent reviews of strained silicon and other references on the topic, see, for example, (Fitzgerald 1995; Schaffler 1997; Brunner 2002; Roberts, Klein et al. 2006; Derbyshire 2007).

Atomistic modeling of $\text{Si}_x\text{Ge}_{1-x}$ by using classical molecular dynamics as well as *ab initio* theories has been reported by many authors. See, for example (Bernard and Zunger 1991; Araki, Fujimura et al. 1997; Goumri-Said, Kanoun et al. 2004; Zhu, Pan et al. 2006; Abtey and Drabold 2007; Torres, Coutinho et al. 2008). The problem with pure atomistic modeling of $\text{Si}_x\text{Ge}_{1-x}$ is that its structure as a function of x is quite uncertain. Whereas the lattice remains essentially cubic, the distribution of the two elements on the diamond lattice sites does not seem to be unique or stable with respect to long range ordering (Qteish and Resta 1988; Qteish and Resta 1988). Yu *et. al* (2001) have shown by using the *ab initio* theory that the two elements are highly miscible. It is therefore a fair assumption that for values of x close to 0 or 1, the elements are randomly distributed and the alloy is quite homogenous. Because of the lack of uniqueness in the distribution of the atoms, it is not possible to develop a purely atomistic model of $\text{Si}_x\text{Ge}_{1-x}$ that can be applicable to all samples of the material. It should be, therefore, useful to develop an averaging scheme for mathematical modeling of $\text{Si}_x\text{Ge}_{1-x}$.

Although it has not been verified experimentally, we expect intuitively that many properties of interest in the strained silicon technology may not be very sensitive to the details of the local atomistic structure. Examples are elastic strains and thermodynamic properties like specific heat and thermal conductivity that are averaged over a finite region of the solid and are also bulk characteristics of the alloy. Since they are averaged over a finite volume of the solid, they would be functions of only x . As long as the alloy remains homogenous, these quantities would not be sensitive to the finer differences in distribution of the atoms over the lattice sites. These are measurable physical quantities that can be used to characterize the alloy and should also be useful in the design calculations for devices based upon the use of strained silicon.

In a recent paper, Torres et al (2008) have carried out detailed *ab initio* calculations on the structure of $\text{Si}_x\text{Ge}_{1-x}$ and tried to predict the average properties of the alloy by averaging over the various supercell structures predicted by the theory. However, the *ab initio* calculations are computationally extensive and lose the rigor of the first principle calculations after averaging. Alternatively one can use a purely continuum model that totally smears out the discrete structure of the lattice and averages all the properties of the solid over the bulk.

The continuum model is useful for modeling the far field elastic response of a solid and also for modeling extended defects such as free surfaces and interfaces. However, it has only a limited validity for lattice statics calculations (Tewary 1973) since it does not account for the dispersive nature of the forces and has a singular behavior at the origin in real space. Moreover, it has no Brillouin zone constraints on the wave vectors and the phonon frequencies, which makes it inadequate for calculation of the frequency spectrum and the thermodynamic quantities. Further, the elastic constants that are the basic parameters of the continuum model need to be related to the atomistic characteristics such as the interatomic potential. There is clearly a need for a simple averaging scheme that can be used to predict the basic elastic and thermodynamic characteristics of $\text{Si}_x\text{Ge}_{1-x}$ for preliminary design calculations.

Our objective is to develop a model for calculating the above averaged characteristics. We propose a semicontinuum Green's function (GF) based model that accounts for the discrete atomistic structure of the lattice in an averaged fashion and uniquely relates it to the bulk continuum characteristics of the solid. It should be more realistic than a pure continuum model for lattice statics modeling because it seamlessly relates the continuum parameters to atomistic interactions. Our proposed model is based upon the lattice GF that accounts for the full Brillouin zone structure of the solid so that it is applicable to nanomaterials. We also utilize the fact that the continuum model is valid in the asymptotic limit and is reasonably applicable to extended defects such as free surfaces and interfaces (Tewary 2004; Tewary and Read 2004; Read and Tewary 2007) that play an important role in nanomaterials.

We model the $\text{Si}_x\text{Ge}_{1-x}$ lattice as a collection of identical hypothetical atoms. The characteristics of each atom are defined to be the weighted averages of the corresponding characteristics of Si and Ge. We will refer to these hypothetical atoms as SxG. The parameters of the interatomic potential between SxG atoms are obtained by interpolating the parameters for Si and Ge and by fitting them with two known physical quantities of the alloy: lattice constant and the cohesive energy. The model predicts elastic constants of the alloy as a function of x . As more data become available, in particular the elastic constants, the model can be refined by

incorporating those data.

For the interatomic potential, we use our recently proposed (Tewary 2011) radial embedded atom model (REAM). This model has been shown to be successful in reproducing seven physical quantities of Si and Ge: cohesive energy, unrelaxed vacancy formation energy, equilibrium lattice constant, Raman frequency, and the three elastic constants. All these quantities are very important for characterization (Mitani, Nakashima et al. 2006; Nakashima, Mitani et al. 2006; Saito, Motohashi et al. 2006) of the solids and lattice statics modeling that includes calculation of lattice distortions, strains and other related elastic properties of the solid. Since the main interest in modeling of strained silicon is in the strains, REAM seems to be a suitable choice for the interatomic potential.

Although the interpolated potential gives the phonon dispersion relations for the solid, our model of hypothetical atoms is not expected to reproduce the details of the actual phonon dispersion of $\text{Si}_x\text{Ge}_{1-x}$. As mentioned earlier, the model can only give those characteristics that can be averaged over a finite region of the solid. We can therefore use the model to calculate the phonon frequency spectrum and the thermodynamic quantities that depend upon the integral of the frequency spectrum but not on the details of the phonon dispersion.

Our model should be useful for calculation of lattice and continuum Green's functions for various thermomechanical and electro-dynamical properties and also for numerical techniques approaches such as meshless Petrov-Galerkin technique for $\text{Si}_x\text{Ge}_{1-x}$ that do not depend upon the detailed local structure of the alloy (Tewary 1973; Liu, Han et al. 2006; Yang and Tewary 2008; Chen, Ke et al. 2009; Yakhno 2011). Moreover, the model gives an effective interatomic potential between SiGe atoms, it can be used for estimating third-order elastic constants using a phonon-based technique (Pham and Tahir Cagin 2010). Because of the asymptotic correspondence between the lattice and the continuum Green's functions, our model should be applicable to multiscale modeling of $\text{Si}_x\text{Ge}_{1-x}$ alloys using standard techniques (Tewary 2004; Tewary and Read 2004; Read and Tewary 2007; Nasdala, Kempe et al. 2010; Ojeda and Cagin 2010). For an excellent review of multiscale modeling in nanomechanics, see (Shen and Atluri 2004).

In this paper we describe the model and quote the relevant formulae for lattice statics modeling of $\text{Si}_x\text{Ge}_{1-x}$. We calculate the three elastic constants c_{11} , c_{12} , and c_{44} of $\text{Si}_x\text{Ge}_{1-x}$ including the effect of internal relaxation for different values of x . We illustrate the method by calculating the displacement field and the strain field at the free surface due to a buried point defect in a semi-infinite $\text{Si}_x\text{Ge}_{1-x}$ alloy for different values of x . Finally, we calculate the radius of curvature of a single-crystal Si substrate of thickness 720 nm with a 49 nm epitaxial film of $\text{Si}(0.846)\text{Ge}(0.154)$ using the anisotropic version of the Stoney formula (Stoney

1909; Janssen, Abdalla et al. 2009). The calculated value of the radius of curvature (312.8 m) is in excellent agreement with a recently measured value (314.5 m), obtained by using the highly precise lattice comparator technique at NIST (Kessler and Vaudin 2011; Vaudin, Kessler et al. 2011). Measurement of wafer curvature is critical to the fabrication of devices in the microelectronics industry. It is an important technique for characterization of elastic properties of nanomaterials and is a part of the NIST program on Standard Reference Materials.

We describe the interatomic potential between SxG atoms in Section 2 based upon the potential derived in an earlier paper (Tewary 2011). We present the calculation of the force constants, the elastic constants, and the lattice GF in Sec. 3 using the harmonic approximation, which is inherent in the GF based models. In Sec. 4, we use the asymptotic limit of the lattice GF to calculate the continuum GF for the Mindlin problem (Pan 2002; Tewary 2004) using the delta function representation (Tewary 2004) and the strains at the free surface of $\text{Si}_x\text{Ge}_{1-x}$ due to a buried point force. Numerical results are given for $x=0$ (pure Ge), 0.2, 0.4, 0.6, 0.8, and 1.0 (pure Si). In Sec. 5, we describe the calculation of curvature of a thin film of $\text{Si}_x\text{Ge}_{1-x}$ on single crystal silicon for $x=0.846$. Finally, the conclusions are summarized in Section 6.

2 Interatomic potential for SxG atoms

We assume that $\text{Si}_x\text{Ge}_{1-x}$ has the perfect diamond cubic lattice structure and all the lattice sites are occupied by SxG atoms. We set up our frame of reference using the Born-von Karman model of a diamond lattice. We label the unit cells by indices L, L' , etc. and an atom inside a unit cell by κ, κ' . The notation for the lattice sites is the same as used in the classic text by Maradudin *et al.* (1971).

We choose the origin of coordinates at an atomic site in the perfect lattice. The Cartesian axes are assumed to be along the crystallographic axes. The Cartesian components will be denoted by the indices i, j ($=1, 2, 3$). Summation convention will be used for Cartesian indices but not for unit cell labels L and κ . Unless stated otherwise, all lengths will be expressed in units of a , where $4a$ is the lattice constant of the solid.

The radius vector of the atom $L\kappa$ is given by

$$\mathbf{R}(L\kappa) = \mathbf{R}(L) + \mathbf{R}'(\kappa), \quad (1)$$

where $\mathbf{R}(L)$ is the radius vector of the unit cell L and $\mathbf{R}'(\kappa)$ is the radius vector of the atom κ with respect to its own unit cell. For diamond lattice, there are two atoms in the unit cell that we label as $\kappa = 0$ and 1. Their radius vectors are $(0, 0, 0)$ and $(1, 1, 1)$, respectively.

We model the interatomic potential between SxG atoms by using REAM (Tewary 2011). We write the energy W of an atom as a sum of two parts: the electronic part ψ that contains the angular terms and a radial part V . Thus for the atom $L\kappa$

$$W(L\kappa) = \psi(L\kappa) + \sum_{L'\kappa'} V(\mathbf{R}(L'\kappa') - L\kappa), \quad (2)$$

where

$$V(r) = A \exp[-\alpha(r/r_0 - 1)] + B \exp[-\beta(r/r_0 - 1)], \quad (3)$$

$r_0 = \sqrt{3}$ is the nearest neighbor distance and A , B , α , and β are parameters to be determined. The range of the interaction is limited to the second neighbor distance. Thus the sum in Eq. (2) extends over all atoms in the first and second neighbor shells. The parameters of REAM (Tewary 2011) are defined in Appendix 1.

In this section we generate the values of the REAM parameters for SxG atoms in $\text{Si}_x\text{Ge}_{1-x}$ for different values of x . The REAM parameters for Si and Ge are quoted in Table 1. The values for $x=0$ and $x=1$ correspond to Si and Ge, respectively. For intermediate values of x , we obtain the parameters by interpolation and fitting the calculated values of the cohesive energy and the equilibrium lattice constants with their known values. The independent parameters are interpolated linearly. The lattice constant and the cohesive energy are interpolated, respectively, using a cubic and quadratic interpolation scheme since their values are known at intermediate values of x . The choice of interpolation formula is of course quite arbitrary. A better interpolation scheme can be developed as more data become available for intermediate values of x .

For the interpolation of α , β , A_E , and $t^{(s)}$ (defined in Appendix 1), we use the following linear formula

$$P_{SG}(x) = P_{SG0}(1 - x) + P_{SG1}x, \quad (4)$$

where P_{SG} is the parameter to be interpolated and P_{SG0} and P_{SG1} are its known values at $x=0$ and 1, respectively.

For the lattice constant we use the following cubic interpolation formula (Dismukes, Ekstrom et al. 1964; Herzog 2000; Arimoto, Yamanaka et al. 2006) that fits the measured values almost exactly:

$$4a(x) = 4a_1x + 4a_0(1 - x) - 0.00436x^2 + 0.0043x^3 + 0.03265x^2 - 0.02829x, \quad (5)$$

where $4a(x)$ is the lattice constant in nm for $\text{Si}_x\text{Ge}_{1-x}$ and $4a_0$ and $4a_1$ are its values for $x=0$ (Ge) and $x=1$ (Si) respectively. For the cohesive energy we use the

quadratic interpolation formula as given below. It fits with the observed values of the cohesive energy E_{C0} at $x=0$ and E_{C1} at $x=1$, and the density function theory result E_{C01} at $x=0.5$ (quoted in (Baskes, Nelson et al. 1989)) corresponding to the binary alloy SiGe.

$$E_C(x) = E_{C1}x + E_{C0}(1 - x) - 4E_{C01}x(1 - x). \quad (6)$$

The variation of the cohesive energy with the concentration is shown in Fig. 1

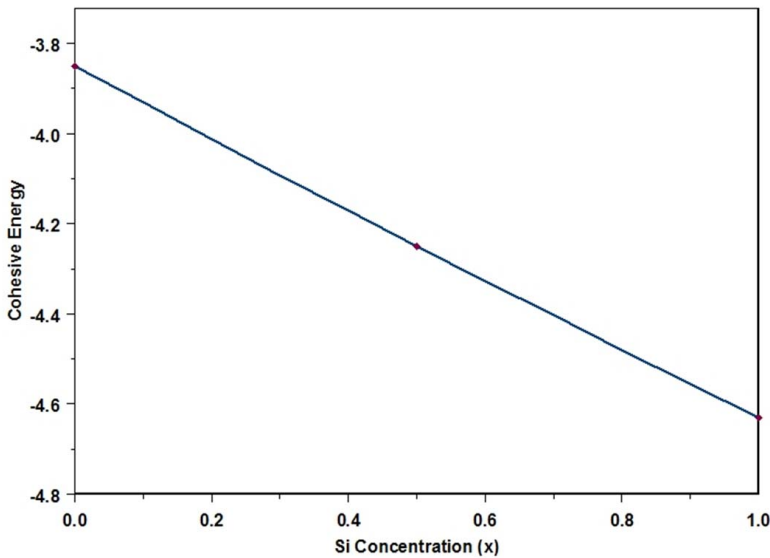


Figure 1: Cohesive energy in eV of $\text{Si}_x\text{Ge}_{1-x}$ as function of x . The points show the experimental values to which the theoretical curve was fitted.

The constants A and B in Eq. (3) are calculated by using the formulae given in Appendix 1 from the interpolated values of α and β and $E_C(x)$ as given by Eq. (6). The values of all the REAM parameters are given in Table 1. The values for intermediate values of x can be obtained by interpolation.

3 Force constants, elastic constants, and Green's function

In this section we give values for the interatomic force constants and expressions for phonon GFs (Maradudin, Montroll et al. 1971). From the phonon GFs we

Table 1: Parameters of REAM. A_E , A, and B are in eV. Other parameters are dimensionless

x	0 (Ge)	0.2	0.4	0.6	0.8	1 (Si)
AE	14.2598	14.4089	14.5581	14.7072	14.8563	15.0055
$\beta(0)$	3.6395	3.8371	4.0346	4.2322	4.4297	4.6273
$\beta(1)$	2.9421	3.1002	3.2583	3.4165	3.5746	3.7327
t(1)	2.2018	2.2080	2.2142	2.2204	2.2265	2.2327
t(2)	2.2142	2.2564	2.2986	2.3408	2.3831	2.4253
α	5.0465	5.2342	5.4218	5.6095	5.7971	5.9848
β	9.5143	9.1903	8.8664	8.5425	8.2186	7.8946
A	-1.9686	-2.2700	-2.6501	-3.1505	-3.8475	-4.9000
B	1.2391	1.5015	1.8442	2.3089	2.9726	3.9943

obtain lattice static and continuum GFs for $\text{Si}_x\text{Ge}_{1-x}$ as functions of x . We then use the GF to calculate the strain at the free surface in a semi-infinite $\text{Si}_x\text{Ge}_{1-x}$ alloy due to a buried point defect.

The force constants $\Phi(L\kappa, L'\kappa')$ between atoms $L\kappa$ and $L'\kappa'$ are obtained by numerical differentiation of the total crystal energy (Maradudin, Montroll et al. 1971). For a perfect lattice the force constants are independent of the choice of the origin and depend upon $L\kappa$ and $L'\kappa'$ only through their difference. They can be, therefore, labeled by a single index $L'\kappa' - L\kappa$. For solids with tetrahedral symmetry, the force constants between the atom at the origin and its first and second neighbor atoms are given below (Herman 1959):

$$\Phi(0, 111) = - \begin{pmatrix} \alpha & \beta & \beta \\ \beta & \alpha & \beta \\ \beta & \beta & \alpha \end{pmatrix} \quad (7)$$

$$\Phi(0, 220) = - \begin{pmatrix} \mu & \nu & \delta \\ \nu & \mu & \delta \\ -\delta & -\delta & \lambda \end{pmatrix} \quad (8)$$

The notation for the force constants is the same as given by Herman (1959). The notation for first neighbor constants should not cause any confusion with that in Eq. (3) since the meaning will be apparent by context. The force constants between the origin and the other atoms in the first and second neighbor shells can be obtained by symmetry (Maradudin, Montroll et al. 1971). The values of the force constants for $\text{Si}_x\text{Ge}_{1-x}$ at several values of x are given in Table 2. We have given the force

constants for more values of x because these are fundamental parameters that are needed in a variety of lattice statics and dynamics calculations.

Table 2: Force constants in eV/a² for Si_xGe_{1-x} for different x . Notation as in Eqs. (7) and (8)

x	α	β	μ	λ	ν	δ
0 (Ge)	6.0229	2.5054	0.3833	-0.4472	0.5216	0.2938
0.1	6.0740	2.5371	0.3950	-0.4588	0.5299	0.2906
0.2	6.1229	2.5654	0.4066	-0.4708	0.5380	0.2872
0.3	6.1698	2.5902	0.4180	-0.4832	0.5458	0.2839
0.4	6.2146	2.6119	0.4292	-0.4960	0.5534	0.2806
0.5	6.2576	2.6304	0.4402	-0.5090	0.5607	0.2773
0.6	6.2988	2.6460	0.4510	-0.5225	0.5676	0.2741
0.7	6.3383	2.6588	0.4614	-0.5362	0.5742	0.2709
0.8	6.3763	2.6690	0.4716	-0.5501	0.5804	0.2679
0.9	6.4128	2.6766	0.4814	-0.5643	0.5861	0.2650
1 (Si)	6.4479	2.6819	0.4909	-0.5787	0.5914	0.2622

The dynamical matrix $\mathbf{D}(\mathbf{K})$ for phonons is defined in terms of the force constants (Maradudin, Montroll et al. 1971), where \mathbf{K} is a wave vector confined to the first Brillouin zone of the lattice. For the diamond structure $\mathbf{D}(\mathbf{K})$ is a 6x6 matrix with its elements labeled by $i\kappa, j\kappa'$ as defined below:

$$D_{ij}(\kappa, \kappa'; \mathbf{K}) = (1/M_x) \sum_L \Phi_{ij}(0\kappa, L\kappa') \exp[-i\mathbf{K} \cdot \mathbf{R}(L\kappa' - 0\kappa)], \tag{9}$$

where M_x is the mass of a S_xG atom obtained by averaging of the masses of Si and Ge atoms using Eq. (4).

The eigenvalues of $\mathbf{D}(\mathbf{K})$ give the phonon frequencies and the phonon dispersion relations. The eigenvalues can be calculated analytically in the high symmetry directions (Herman 1959). As mentioned earlier, our model is not expected to give the details of the phonon dispersion. However, the low \mathbf{K} limit of the phonon dispersion in the symmetry directions gives valuable relations between the force constants and the elastic constants using the method of the long waves, which accounts for the internal relaxation in a non-Bravais lattice. For the diamond lattice structure, these relations have been derived by Herman (1959).

The variations of three elastic constants for Si_xGe_{1-x} with x are shown in Fig. 2. We see from the figure that the dependence of all the three elastic constants on concentration is almost linear. Interestingly, this is as predicted by the simple rule

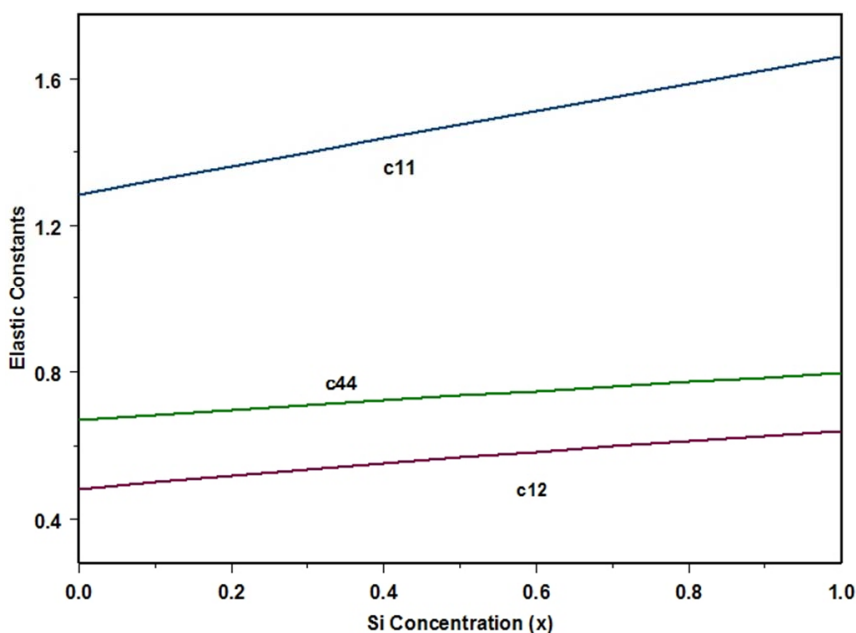


Figure 2: Calculated elastic constants in 100 GPa of $\text{Si}_x\text{Ge}_{1-x}$ as function of x .

of mixtures, which is in reasonable agreement with the measured values (Baker and Arzt 2000) within experimental errors.

To obtain a quantitative comparison, our calculated values of the elastic constants for SiGe ($x=0.5$) in GPa are $c_{11}=147$, $c_{12}=59$ and $c_{44}=73$ as shown in Fig. 2. The corresponding values measured by Mendik et. al (1991) for Si(0.49)Ge(0.51) are $c_{11}=137.7 \pm 3.3$, $c_{12}=51.2 \pm 4.0$, and $c_{44}=66.6 \pm 2.0$. The measured values (Baker and Arzt 2000) for $x=1$ (Si) are $c_{11}=165.8$, $c_{12}=63.9$, $c_{44}=79.6$ and for $x=0$ (Ge) $c_{11}=128.5$, $c_{12}=48.3$ and $c_{44}=66.8$. The measured value of c_{44} for Si(0.49)Ge(0.51) is obviously inconsistent with the values for pure Si and pure Ge. Mendik et al (Mendik, Ospelt et al. 1991) have also given their measured values for a SiGe superlattice. These values are $c_{11}=147 \pm 3.6$, $c_{12}=59.0 \pm 4.2$, $c_{44}=73.0 \pm 2.2$. These values are in almost exact agreement with our theoretical values given above and in Fig. 2. We infer therefore that our semi-continuum model and our effective potential between SxG atoms is reasonably reliable for estimating the elastic properties of $\text{Si}_x\text{Ge}_{1-x}$ solids.

Our interest in this paper is in the lattice statics GF (Tewary 1973). It is obtained

from the phonon GF (Maradudin, Montroll et al. 1971), which is defined below:

$$G_{ij}(\omega^2; 0\kappa, L\kappa') = (1/N)\sum_K G_{ij}(\kappa, \kappa'; \omega^2, \mathbf{K}) \exp[i\mathbf{K}\cdot\mathbf{R}(L\kappa' - 0\kappa)], \quad (10)$$

where $\iota = \sqrt{-1}$, N is the total number of unit cells, \mathbf{I} is the 6x6 identity matrix, ω is the phonon frequency, and $\mathbf{G}(\mathbf{K})$ is the Fourier transform of the GF matrix defined as follows:

$$\mathbf{G}(\omega^2, \mathbf{K}) = (1/M_x)[- \omega^2 \mathbf{I} + \mathbf{D}(\mathbf{K})]^{-1}, \quad (11)$$

The sum in Eq. (10) is over all the \mathbf{K} -vectors in the first Brillouin zone of the lattice. The eigenvalues of $\mathbf{D}(\mathbf{K})$ must be real for the lattice to be stable. Hence, it is apparent from Eq. (11), that the phonon GF has singularities on the real axis. A suitable contour needs to be defined for the evaluation of the GF (Maradudin, Montroll et al. 1971). For this purpose, it is convenient to add a small imaginary part to ω^2 and take the limit as the imaginary part approaches zero. The phonon frequency spectrum is then given by the imaginary part of the diagonal elements of the GF as given below (Maradudin, Montroll et al. 1971):

$$g(\omega) = 2\omega \text{ImTr} \sum_K \mathbf{G}(\omega^2 - \iota 0_+, \mathbf{K}), \quad (12)$$

where $\iota 0_+$ indicates that the limit of the zero imaginary part is approached from the positive side.

The frequency spectrum is a very important characteristic of the solid. It is needed for calculation of free energy, specific heat, Debye-Waller factor, phase diagrams, scattering cross-sections, *etc.* All these quantities are useful in characterizing Si_xGe_{1-x} alloys. These calculations will be presented in a later paper.

The lattice statics GF \mathbf{U} of a solid is defined as the zero frequency limit of the phonon GF (Tewary 1973). From Eq. (10), we obtain the following expression for \mathbf{U} :

$$U_{ij}(L\kappa, L'\kappa') = (1/N)\sum_K G_{ij}(\kappa, \kappa'; \mathbf{K}) \exp[i\mathbf{K}\cdot\mathbf{R}(L'\kappa' - L\kappa)], \quad (13)$$

where

$$\hat{\mathbf{U}}(\mathbf{K}) = \text{Lim}_{\omega \rightarrow 0} \mathbf{G}(\omega^2, \mathbf{K}) = [\Phi(\mathbf{K})]^{-1}, \quad (14)$$

and $\Phi(\mathbf{K})$ is the Fourier transform of the force constant matrix as defined in Eq. (10). Note that the lattice statics GF is independent of the atomic mass.

In the near field region, we can calculate the discrete lattice GF directly from Eq. (13). Methods for calculation of the lattice GF and its application for solving the

defect problem in lattices have been described in detail in (Tewary 1973; Thomson, Zhou et al. 1992). The lattice GF accounts for discrete lattice effects and is applicable to calculation of lattice distortions in the entire lattice. However, the present model is an averaged model and is therefore not expected to reproduce the finer details of the discrete atomistic effects.

In the asymptotic or far field region, we can use the semicontinuum approximation by utilizing the fact that the asymptotic limit (Tewary 1973) of \mathbf{U} for large $R(L\kappa-L'\kappa')$ is the continuum GF. In the continuum limit, we replace the summation over \mathbf{K} by an integral in Eq. (13) and use the low- \mathbf{K} limit of $\Phi(\mathbf{K})$. Only the acoustic part of $\Phi(\mathbf{K})$ contribute to the continuum GF, which is simply the Christoffel matrix defined as follows:

$$\Lambda_{ij}(\mathbf{K}) = c_{ikjl}K_kK_l, \quad (15)$$

where \mathbf{c} is the fourth rank elastic constant tensor. Thus, in the continuum limit, we obtain

$$\hat{\mathbf{U}}_0(\mathbf{K}) = [\Lambda(\mathbf{K})]^{-1}, \quad (16)$$

and

$$\mathbf{U}_{0ij}(\mathbf{R}) = (1/2\pi)^3 \int_{-\infty}^{\infty} \hat{\mathbf{U}}_{0ij}(\mathbf{K}) \exp(i\mathbf{K}\cdot\mathbf{R}) d\mathbf{K}, \quad (17)$$

apart from the normalization factors in the definition of $\hat{\mathbf{U}}_0(\mathbf{K})$. The subscript 0 indicates that no boundary conditions have been applied to the GF and it is valid only for the infinite vector space. The continuum GF is applicable to extended defects such as free surfaces and interfaces by applying appropriate boundary conditions. Powerful techniques for calculating the continuum GF for anisotropic solids for different boundary conditions corresponding to free surfaces and interfaces are available in the literature (Tewary, Wagoner et al. 1989; Pan 2002; Yang and Pan 2002; Tewary 2004; Tewary and Read 2004; Yang and Tewary 2005; Yang and Tewary 2006; Read and Tewary 2007; Yang and Tewary 2007).

Now we apply the lattice statics GF to calculate the strain field in the solid due to a substitutional point defect. We assume that the point defect is at the origin. A point defect may be a vacancy or a foreign atom. We can also model a small local variation in the concentration x as a distribution of point defects. In a perfect lattice, the force at each atom in the lattice is zero. The effect of the point defect is to introduce forces at the lattice sites near the defect and also to change the GF. It is possible to account for the change in the GF by defining effective Kanzaki forces

(Tewary 1973; Tewary 2004; Read and Tewary 2007) and use the perfect lattice GF along with the Kanzaki force. If we denote the Kanzaki force at $L\kappa$ by \mathbf{F}_K , the displacement field \mathbf{u} is given by (Tewary 1973)

$$\mathbf{u}(L\kappa) = \sum_{L'\kappa'} \mathbf{U}_0(L\kappa, L'\kappa') \mathbf{F}_K(L'\kappa') \quad (18)$$

The Kanzaki force due to a substitutional defect follows the symmetry of the lattice. If we restrict the forces to the nearest neighbors of the defect, then the form of the vector $\mathbf{F}(L'\kappa')$ for the atom $L'\kappa' = (1, 1, 1)$ is

$$\mathbf{F}_K(1, 1, 1) = (f, f, f), \quad (19)$$

where

$$f = \partial \Delta W / \partial u_1(1, 1, 1), \quad (20)$$

ΔW is the change in the crystal energy due to the defect, and the derivative in Eq. (20) is evaluated at $u_1(L'\kappa' = 1, 1, 1)$. The force vectors for other atoms in the nearest neighbor shell can be written by symmetry.

In the near field region the atomistic displacements can be calculated from Eq. (18) by using the lattice GF defined by Eq. (13). These displacements must be treated as average lattice distortion over a finite region. In the semicontinuum approximation, we calculate the force f by using the discrete interatomic potential but use the continuum GF approximation for \mathbf{U} . The approximation is valid for $|\mathbf{R}(L\kappa - L'\kappa')| \gg \mathbf{R}(L'\kappa')$ and also for extended defects such as free surfaces and interfaces (Tewary 2004).

One advantage of using the semicontinuum approximation is that \mathbf{R} and \mathbf{u} become continuous and differentiable variables. Hence, their derivatives are well defined (Read and Tewary 2007). These derivatives are needed for calculation of the continuum parameters such as stress and strains. In a purely discrete model, \mathbf{R} and \mathbf{u} are discrete variables so the definitions of the derivatives and therefore the stresses and strains are somewhat subjective. In the next section we shall apply Eq. (18) to calculate the strain and the displacement fields due to a buried defect at a free surface in $\text{Si}_x\text{Ge}_{1-x}$.

4 Strain field on the free surface of $\text{Si}_x\text{Ge}_{1-x}$ due to a buried point defect

For the purpose of illustration, we apply our model to a semi-infinite $\text{Si}_x\text{Ge}_{1-x}$ alloy containing a buried point defect as described in the previous section. We calculate the strains at the surface due to the defect and the displacement field at the free surface. The continuum form of the GF is especially convenient for simulating a

free surface by applying appropriate boundary conditions. The present case of a buried point defect in a semi-infinite solid is the Mindlin problem. Efficient methods for solving the Mindlin and similar problems for anisotropic solids have been developed by Pan, Yang, and their collaborators (Pan and Yuan 2000; Pan and Yang 2001; Pan 2002; Yang and Pan 2002; Pan and Yang 2003). We shall, however, use a slightly different technique based upon the delta function representation of the GF (Tewary 2004).

We assume that the free surface is the (001) plane. For these calculations it is more convenient to choose a frame of reference in which the origin and the X- and Y-axes are on the free surface and the positive Z-axis points into the solid.

In the continuum approximation we replace the variable $\mathbf{R}(L\kappa-L'\kappa')$ by a continuous vector variable \mathbf{r} with Cartesian components x_1 , x_2 and x_3 along the X, Y, and Z directions respectively. The atomic sites $L'\kappa'$ where the Kanzaki force is applied are still treated as discrete sites. The field points $L\kappa$ are confined to the free surface. The displacement field at the free surface is now given by the continuum form of Eq. (18) as given below

$$\mathbf{u}(\mathbf{r}_s) = \sum_{L'\kappa'} g_c(\mathbf{r}_s, \mathbf{L}'\kappa') \mathbf{F}_K(\mathbf{L}'\kappa'), \quad (21)$$

where \mathbf{r}_s is a continuous variable on the free surface ($x_3=0$) and U_c is the continuum GF that satisfies the prescribed boundary conditions for the Mindlin problem. The zero-traction boundary condition at the free surface, which is the plane at $x_3=0$, is given by

$$\tau_{i3}(\mathbf{r}) = c_{i3jk} e_{jk}(\mathbf{r}) = 0 (x_3 = 0), \quad (22)$$

where

$$e_{jk}(r) = \partial u_j(\mathbf{r}) / \partial x_k, \quad (23)$$

and \mathbf{e} and $\boldsymbol{\tau}$ denote respectively the second-rank strain and stress tensors. The off-diagonal elements of Eq. (23) have to be symmetrized in the definition of the strain tensor.

We consider a point defect at a depth h below the surface so the coordinates of the defect are (0,0,- h). The coordinates of its four nearest neighbors are (1,1,1+ h), (-1,-1,1+ h), (-1,1,-1+ h), and (1,-1,-1+ h). These are the only atoms for which the Kanzaki force is non-zero. The continuum Green's function \mathbf{U}_c that satisfies Eq. (22) is given below. It is written as a sum of \mathbf{U}_0 , the Green's function for the infinite solid, and \mathbf{U}_s due to the contribution of the free surface, as follows:

$$\mathbf{U}_c(\mathbf{r}, L\kappa) = \mathbf{U}_0(\mathbf{r}-\mathbf{R}(L\kappa)) + \mathbf{U}_s(\mathbf{r}, \mathbf{R}(L\kappa)), \quad (24)$$

where $L\kappa$ is confined to the four discrete lattice sites for which $\mathbf{F}(L\kappa)$ is nonzero. The first term on the RHS of (24) gives the GF for an infinite solid, and the second term represents the correction due to the free surface. Since the first part has translation symmetry, it depends upon \mathbf{r} and \mathbf{R} only through their difference. The second part depends upon the two variables separately. The full form of \mathbf{U}_c , the GF for the Mindlin problem (Tewary 2004), is given in Appendix 2.

The displacement field at any \mathbf{r} is given by Eq. (21) and the strain field can be calculated by using (23). The X and Z components u_1 and u_3 of the displacement field for \mathbf{r} along the X axis ($r_2=r_3=0$) at the free surface for different values of the concentration x are shown in Figures 3 and 4, respectively. The corresponding strain components e_{11} and e_{33} are shown in Figures 5 and 6, respectively. In these calculations we have assumed $f=1$ nN which is the approximate value of the force due to a substitutional defect of the same kind as Si or Ge. The depth of the defect below the free surface was assumed to be 10.

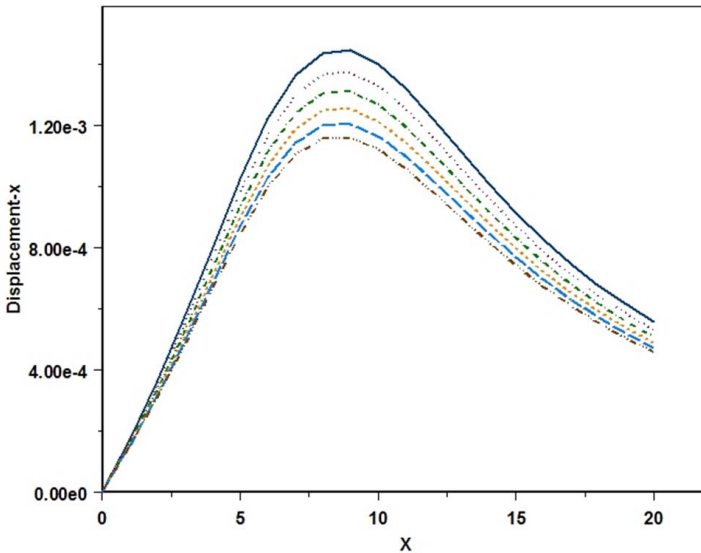


Figure 3: X-component of the displacement field at the free surface of semi-infinite $\text{Si}_x\text{Ge}_{1-x}$ along the X axis ($X,0,0$) as function of X for various values of the Ge concentration x . All lengths are in units of a . Legend: Solid line for $x=0$ (pure Ge); dots for $x=0.2$; dash dots for $x=0.4$; dashes for $x=0.6$; long dashes for $x=0.8$; dash and three dots for $x=1.0$ (pure Si).

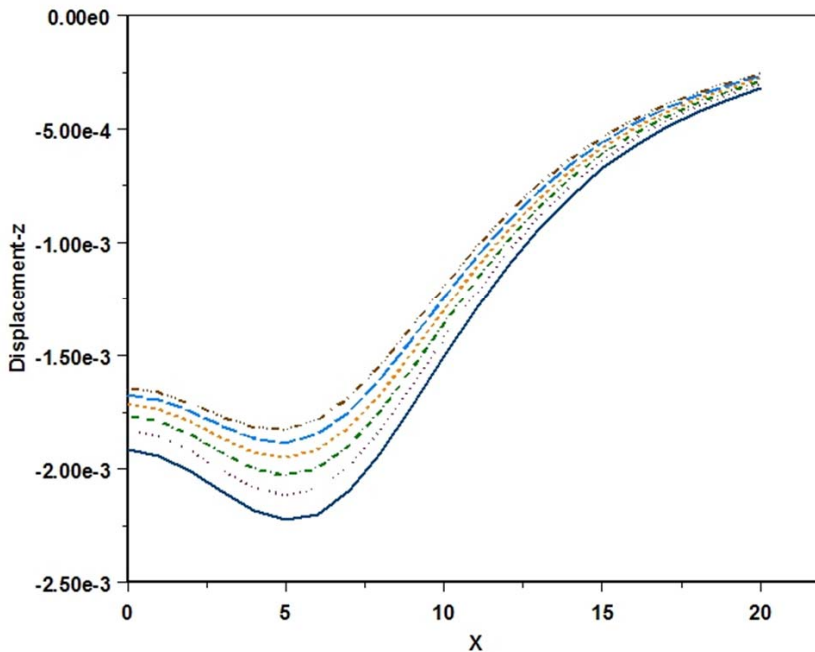


Figure 4: Z-component of the displacement field at the free surface of semi-infinite $\text{Si}_x\text{Ge}_{1-x}$ along the X axis ($X,0,0$) as function of X for various values of the Ge concentration x . Notation and units same as in Fig. 3.

We see from Figs. 3 and 4 that the magnitude of the displacement field first increases and then decreases as X increases with an extremum at about $X=10$ for the X component and at about $X=5$ for the Z component. The X-component of the displacement field is 0 at $X=0$ due to the symmetry. The extremum is a consequence of the lattice anisotropy because the Green's function depends upon the distance as well as the direction of the source and the field points. The distribution of forces at 4 lattice sites around the defect forms a quadrupole at the defect. The extremum occurs at a point where the total of the projection of the Green's function tensor has an extremum. The curve in Fig. 4 shows the formation of a hump at the surface immediately above the defect. This is similar to the hump due to a Ge quantum dot in silicon as calculated in an earlier paper (Read and Tewary 2007). The qualitative behavior of the strain curves shown in Figs. 5 and 6 can be understood in a similar way. These curves should be measurable and can be useful for characterization of the alloy.

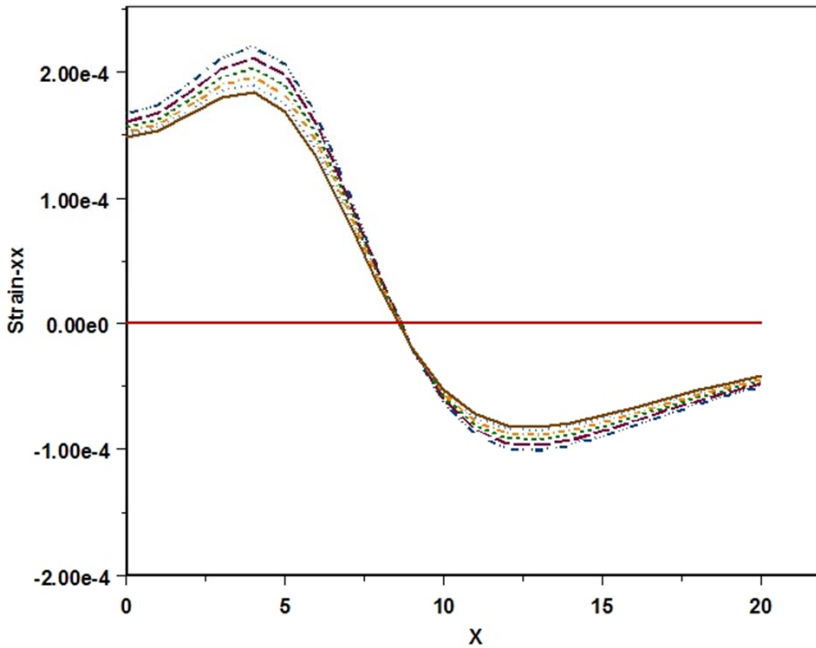


Figure 5: XX-component of the strain tensor at the free surface of semi-infinite $\text{Si}_x\text{Ge}_{1-x}$ along the X axis $(X,0,0)$ as function of X for various values of the Ge concentration x. Notation and units same as in Fig. 3

5 Calculation of curvature of a Si substrate with a film of $\text{Si}_x\text{Ge}_{1-x}$

We now use the elastic constants derived for $\text{Si}_x\text{Ge}_{1-x}$ to calculate the curvature of a single-crystal Si substrate of thickness 720 nm with a 49 nm epitaxial film of $\text{Si}(0.846)\text{Ge}(0.154)$ and compare the calculated value with the value measured recently at NIST (Kessler and Vaudin 2011; Vaudin, Kessler et al. 2011). There is a strong industrial interest in modeling and measurement of wafer curvatures. Wafer curvature measurements are critical to fabrication of devices because wafers must be flat within a certain tolerance. It is also an important technique for characterization of the elastic properties of nanomaterials and is a part of the NIST program on Standard Reference Materials. The curvature is experimentally determined by measuring the spatial variation of the orientation of the lattice planes across a surface (Vaudin, Kessler et al. 2011). The measurement technique, developed at NIST, is based upon the use of lattice comparator that can determine the orientation of lattice planes perpendicular to a curved crystal surface very precisely with an accuracy of $2 \cdot 10^{-9}$ rad (Vaudin, Kessler et al. 2011).

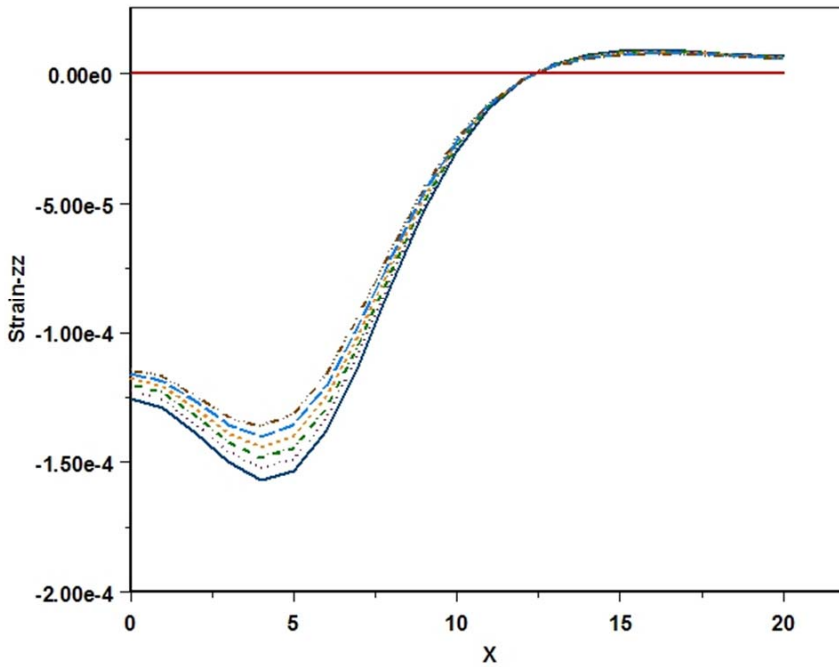


Figure 6: ZZ-component of the strain tensor at the free surface of semi-infinite $\text{Si}_x\text{Ge}_{1-x}$ along the X axis (X,0,0) as function of X for various values of the Ge concentration x. Notation and units same as in Fig. 3

When a thin film is deposited on a substrate, it induces a curvature due to the stresses caused by the mismatch between the lattice constants of the film and the substrate. This stress has been calculated in the classic paper by Stoney (1909) for isotropic solids. The curvature of the composite can be derived from Stoney's equation and is given by (Freund, Floro et al. 1999; Vaudin, Kessler et al. 2011)

$$1/R_c = 6(M_f/M_s)\epsilon_m(h_f/h_s^2), \quad (25)$$

where

$$\epsilon_m = (a_f - a_s)/a_s, \quad (26)$$

is the lattice mismatch, R_c is the radius of curvature (ROC), and M and h denote, respectively, the effective elastic modulus and the thickness of the film or the substrate. The quantities for the film and the substrate are identified by the subscripts f and s, respectively. The values of $a_{f,s}$ are calculated by using Eq. (5).

It has been shown by Janssen et al. (2009) that the form of the Stoney's equation is also valid for anisotropic solids with the appropriate definition of the elastic moduli $M_{f,s}$. For an anisotropic cubic solid with the interface on the (001) plane, the effective modulus is given by (Janssen, Abdalla et al. 2009)

$$M = c11 + c12 - 2(c12^2)/c11. \quad (27)$$

We now calculate R_c by using our model for $\text{Si}_x\text{Ge}_{1-x}$ for $x=0.154$, the alloy for which the curvature has been measured. The calculated values of the parameters in the force constant matrices for the first and second neighbor atoms for $x=0.154$, as defined in Eqs. (7) and (8), are given below in the units of $\text{eV}/\text{\AA}^2$:

I neighbors: $\alpha = 6.39323$, $\beta = 2.67278$

II neighbors: $\mu=0.47613$, $\lambda = -0.55663$, $\nu = 0.58308$, and $\delta=0.26654$

These values yield the following values of the elastic constants of the alloy in the units of GPa:

$c11=160.2$, $c12=61.9$, and $c44=77.8$.

The elastic constants of Si substrate are given in Sec. 3. The lattice constant of $\text{Si}_x\text{Ge}_{1-x}$, as derived from Eq. (5), is 5.4627 \AA and is 5.431 \AA for Si. This gives $\epsilon_m=5.837 \times 10^{-3}$ from Eq. (26). Finally, using all the above values, we obtain from Eq. (25) $R_c = 312.8 \text{ m}$.

The measured value of R_c as reported by Vaudin *et al.* (2011) is about 275 m . However, a very recent and accurate measurement (Kessler and Vaudin 2011) gives $R_c = 314.5 \text{ m}$ which is in excellent agreement with our calculated value 312.8 m .

6 Conclusions

We have proposed a semicontinuum GF based model for analysis of averaged mechanical characteristics of $\text{Si}_x\text{Ge}_{1-x}$. The model is semicontinuum in the sense that the forces are distributed at discrete lattice sites but the GF is approximated by the continuum GF asymptotically and by averaged lattice GF in the near field. The averaging is achieved by replacing Si and Ge atoms by identical hypothetical atoms called SxG that are hybrids of x fraction Si and $(1-x)$ fraction of Ge. The force constants for the lattice GF and the elastic constants for the continuum GF are derived from the interatomic potential between the SxG atoms, which is obtained from the REAM (radial embedded atom model) proposed in an earlier paper. The model predicts correct values of the elastic constants of SiGe ($x=0.5$), which gives at least some credence to the model.

For the purpose of illustration we have applied the model to a semi-infinite $\text{Si}_x\text{Ge}_{1-x}$ alloy containing a point defect. We have calculated the displacement and the strain

field at the free surface of the alloy for $x=0$ (pure Ge), 0.2, 0.4, 0.6, 0.8, and 1.0 (pure Si) due to a point defect at depth 10 below the free surface. These are measurable quantities. The displacement field at the free surface shows a hump which is a characteristic of the lattice anisotropy. This should, in principle, be observable. Finally, using the elastic constants predicted by our model, we have calculated the radius of curvature of a single-crystal Si substrate of thickness 720 nm, induced by a 49 nm epitaxial film of Si(0.846)Ge(0.154). The calculated value 312.8 m is in excellent agreement with the recently measured value 314.5 m at our laboratory. Measurement of wafer curvature is critical to the fabrication of devices in the microelectronics industry and is an important technique for characterization of the elastic properties of nanomaterials.

The model is somewhat similar to the multiscale GF model (Tewary 2004; Tewary and Read 2004; Read and Tewary 2007) developed earlier. The main difference is that in the multiscale model the Kanzaki force is calculated by using molecular dynamics without making the linear approximation, and both lattice and continuum GF are used in the calculation of the displacements. One advantage of the semicontinuum model is that the continuum parameters like strains are well defined since the displacement field is continuous and differentiable. The definition of strain in the discrete lattice theory is somewhat arbitrary.

Although not considered in this paper, the model should be applicable for calculation of thermodynamic properties. An expression for the phonon frequency distribution function has been given that can be used for thermodynamic calculations.

The main uncertainty in the proposed model is in the values of the REAM parameters arising from the interpolation scheme used in estimating the parameters. The only test of reliability of the parameters is that they predict the correct values of elastic constants for SiGe ($x=0.5$) and the curvature of the composite film. This is an important test but still a rather limited test. If measured values of the strain and the displacement fields at the free surface, and more refined measurements of elastic constants and cohesive energy for different values of x were available, they could provide more reliable values of the REAM parameters. Measurement of thermodynamic quantities such as specific heat and thermal conductivity would also help in getting better estimates of the parameters.

Appendix 1: Parameters of REAM

The electronic part of the REAM potential (Tewary 2011) in Eq. (2) is given by

$$\psi(L\kappa) = E(\rho(L\kappa)) - E0(L\kappa), \quad (28)$$

where

$$E(\rho(L\kappa)) = A_E \rho(L\kappa) \ln \rho(L\kappa), \tag{29}$$

$$\rho(L\kappa) = (2\rho^{(0)}(L\kappa)/Z)[1 + \exp(-\Gamma)]^{-1}, \tag{30}$$

$$\Gamma(L\kappa) = (1/\rho^{(0)}(L\kappa))^2 [\sum_{s=1,2} t^{(s)}(\rho^{(s)}(L\kappa))^2], \tag{31}$$

$$\rho^{(0)}(L\kappa) = \sum_{L'\kappa'} \rho^{a(0)}(R(L'\kappa' - L\kappa)), \tag{32}$$

$$[\rho^{(1)}(L\kappa)]^2 = \sum_i [\sum_{L'\kappa'} X_i(L'\kappa' - L\kappa) \rho^{a(1)}(R(L'\kappa' - L\kappa))]^2, \tag{33}$$

$$[\rho^{(2)}(L\kappa)]^2 = \sum_{ij} [\sum_{L'\kappa'} X_i(L'\kappa' - L\kappa) X_j(L'\kappa' - L\kappa) \rho^{a(2)}(R(L'\kappa' - L\kappa))]^2 - (1/3) [\sum_{L'\kappa'} \rho^{a(2)}(R(L'\kappa' - L\kappa))]^2, \tag{34}$$

$$\rho^{a(s)}(r) = \exp[-\beta^{(s)}(r/R_0 - 1)] \quad (s = 0, 1, \text{ or } 2), \tag{35}$$

$$X_i(L'\kappa' - L\kappa) = R_i(L'\kappa' - L\kappa) / |R(L'\kappa' - L\kappa)|, \tag{36}$$

$$E_0 = (1/Z) \sum_{L'\kappa'} E[\rho^{a(0)}(|R(L'\kappa' - L\kappa)|)], \tag{37}$$

The constants A and B in Eq. (3) are related to α , β , and the cohesive energy E_C of the solid as follows:

$$A = E_C P_{22} / D_t, \tag{38}$$

$$B = -E_C P_{21} / D_t, \tag{39}$$

$$P_{11} = 4[1 + 3\exp(-\alpha q)], \tag{40}$$

$$P_{12} = 4[1 + 3\exp(-\beta q)], \tag{41}$$

$$P_{21} = 4\alpha[1 + 3(1 + q)\exp(-\alpha q)], \tag{42}$$

$$P_{22} = 4\beta[1 + 3(1 + q)\exp(-\beta q)], \tag{43}$$

$$D_t = P_{11}P_{22} - P_{12}P_{21}, \tag{44}$$

where $q = 2\sqrt{2/3}$. Equations (38) and (39) have been derived by using the condition that W is minimum at the equilibrium value of the lattice constant and equal to E_C .

Appendix 2: Green’s function for the Mindlin problem

In this appendix we give the expression for U_c in Eq. (24), which is the GF for the Mindlin problem. It satisfies the boundary condition given by Eq. (22). Only the results are given here. For derivation, see (Tewary 2004).

We define a 2D vector χ in the (X,Y) subspace of \mathbf{r} such that $\chi_1 = x_1$ and $\chi_2 = x_2$. We can thus write the general 3D vector \mathbf{r} as (χ, x_3) . In an analogous manner, we also define the corresponding 2D vectors \mathbf{q} and ρ in the subspaces of \mathbf{K} and \mathbf{R} , respectively, such that $\mathbf{K} = (\mathbf{q}, K_3)$ and $\mathbf{R} = (\rho, R_3)$, where $\kappa_1 = K_1$, $\kappa_2 = K_2$, $r_1 = R_1$, and $r_2 = R_2$. Further we specify \mathbf{q} to be a unit vector defined as follows:

$$K_1 = q_1 = \cos(\theta); \quad K_2 = q_2 = \sin(\theta); \quad -\infty \leq K_3 \leq \infty \text{ and } 0 \leq \theta \leq 2\pi. \quad (45)$$

The two terms in Eq. (24) are given below:

$$U_0(\chi - \mathbf{R}) = Re(1/4\pi^2) \int d\theta \sum_m \mathbf{M}(\mathbf{q}, \bar{Q}_m) \bar{W}_m M_0(\mathbf{q}, Q_m, \mathbf{R}), \quad (46)$$

$$U_s(\chi, \mathbf{R}) = -Re(1/4\pi^2) \int d\theta \sum_{m,n} \mathbf{V}(\mathbf{q}, Q_m, Q_n) M_s(\mathbf{q}, Q_m, Q_n, \mathbf{R}), \quad (47)$$

$$M_0(\mathbf{q}, Q_m, \mathbf{R}) = [\mathbf{q} \cdot (\chi - \rho) + \bar{Q}_m(x_3 - R_3) + i\epsilon]^{-1}, \quad (48)$$

$$M_s(\mathbf{q}, Q_m, Q_n, \mathbf{R}) = [\mathbf{q} \cdot (\chi - \rho) + Q_m x_3 - \bar{Q}_n R_3 + i\epsilon]^{-1}, \quad (49)$$

$$\mathbf{V}(\mathbf{q}, Q_m, Q_n) = \mathbf{M}(\mathbf{q}, Q_m) \mathbf{A}(\mathbf{q}) \mathbf{S}(\mathbf{q}, \bar{Q}_n) \mathbf{M}(\mathbf{q}, \bar{Q}_n) W_m \bar{W}_n, \quad (50)$$

$$\mathbf{A}(\mathbf{q}) = [\sum_m \mathbf{S}(\mathbf{q}, Q_m) \mathbf{M}(\mathbf{q}, Q_m) W_m]^{-1}, \quad (51)$$

$$S_{ij}(\mathbf{q}, K_3) = c_{i3jk} K_k, \quad (52)$$

$$W_m = 1/[2c_{11}c_{44}Q_m \prod_{n \neq m} (Q_m^2 - Q_n^2)], \quad (53)$$

where the overhead bar denotes complex conjugate, Q_m and Q_n ($m, n = 1, 3$) are three roots of the polynomial equation in K_3 ,

$$P(\mathbf{q}, K_3) = 0, \quad (54)$$

and $P(\mathbf{K})$ is the determinant of the Christoffel matrix $\Lambda(\mathbf{K})$ defined by Eq. (15).

Equation (I-20) has 6 roots that are functions of θ . We choose three roots with positive imaginary parts. The integral over θ in Eqs. (46) and (47) is carried out in the interval 0 to 2π which can be reduced by using symmetry. Equation (24) gives the continuum GF for a semi-infinite solid that satisfies the Mindlin boundary condition. It requires only a one-dimensional numerical integration over θ , which is rapidly convergent.

References

- Abtew, T. A. and D. A. Drabold** (2007). Ab initio models of amorphous $\text{Si}_{1-x}\text{Ge}_x$: H. *Physical Review B* **75**(4).
- Araki, T., N. Fujimura and T. Ito** (1997). The stability of ordered structures in SiGe films examined by strain-energy calculations. *Journal of Crystal Growth* **174**(1-4): 675-679.
- Arimoto, K., J. Yamanaka, K. Nakagawa, K. Sawano, Y. Shiraki, S. Koh and N. Usami** (2006). Determination of lattice parameters of SiGe/Si(110) heterostructures. *Thin Solid Films* **508**(1-2): 132-135.
- Baker, S. P. and E. Arzt** (2000). Elastic stiffness constants of SiGe. *Silicon Germanium and SiGe: Carbon*. E. Kasper and K. Lyutovich. London, INSPEC, IEE: 91-93.
- Baskes, M. I., J. S. Nelson and A. F. Wright** (1989). Semiempirical modified embedded-atom potentials for silicon and germanium. *Physical Review B* **40**(9): 6085-6100.
- Bernard, J. E. and A. Zunger** (1991). Strain-Energy and Stability of Si-Ge Compounds, Alloys, and Superlattices. *Physical Review B* **44**(4): 1663-1681.
- Brunner, K.** (2002). Si/Ge nanostructures. *Reports on Progress in Physics* **65**(1): 27-72.
- Chen, J.-T., J.-N. Ke and H.-Z. Liao** (2009). Construction of Green's function using null-field integral approach for Laplace problems with circular boundaries *CMC: Computers, Materials, & Continua* **9**: 93-110.
- Derbyshire, K.** (2007). Stretching silicon mobility with strain engineering. *Solid State Technology* **50**(3): 38-41.
- Dismukes, J. P., L. Ekstrom and P. R.J.** (1964). Lattice Parameter and Density in Germanium-Silicon Alloys. *Journal of Physical Chemistry* **68**: 3021-3027.
- Fitzgerald, E. A.** (1995). GeSi/Si Nanostructures. *Annual Review of Materials Science* **25**: 417-454.
- Freund, L. B., J. A. Floro and E. Chason** (1999). Extensions of the Stoney formula for substrate curvature to configurations with thin substrates or large deformations. *Applied Physics Letters* **74**(14): 1987-1989.
- Goumri-Said, S., M. B. Kanoun, A. E. Merad, G. Merad and H. Aourag** (2004). Empirical molecular dynamics study of structural, elastic and thermodynamic properties of zinc-blende-like SiGe compound. *Materials Science and Engineering B-Solid State Materials for Advanced Technology* **111**(2-3): 207-213.
- Herman, F.** (1959). Lattice vibrational spectrum of germanium. *Journal of Physics*

and *Chemistry of Solids* **8**: 405-418.

Herzog, H. J. (2000). Crystal structure, lattice parameters and liquidus-solidus curve of the SiGe system. *Silicon Germanium and SiGe: Carbon*. E. Kasper and K. Lyutovich. London, INSPEC, IEE: 45-49.

Janssen, G. C. A. M., M. M. Abdalla, F. van Keulen, B. R. Pujada and v. V. B. (2009). Celebrating the 100th anniversary of the Stoney equation for film stress: Developments from polycrystalline steel strips to single crystal silicon wafers. *Thin Solid Films* **517**: 1858-1867.

Kessler, E. G. and M. D. Vaudin (2011). Private Communication; to be published.

Liu, H. T., Z. D. Han, A. M. Rajendran and S. N. Atluri (2006). Computational Modeling of Impact Response with the RG Damage Model and the Meshless Local Petrov-Galerkin (MLPG) Approaches *CMC: Computers, Materials, & Continua* **4**: 43-54.

Maradudin, A. A., E. W. Montroll, G. H. Weiss and I. P. Ipatova, Eds. (1971). *Theory of lattice dynamics in the harmonic approximation*. Solid State Physics. New York, Academic Press.

Mendik, M., M. Ospelt, H. von Kanel and P. Wachter (1991). Determination of elastic properties of Si/Ge superlattices and Si(1-x) Ge_x films from surface acoustic modes by Brillouin scattering. *Applied Surface Science* **50**: 303-307.

Mitani, T., S. Nakashima, H. Okumura and A. Ogura (2006). Depth profiling of strain and defects in Si/Si_{1-x}Ge_x/Si heterostructures by micro-Raman imaging. *Journal of Applied Physics* **100**(7).

Nakashima, S., T. Mitani, M. Ninomiya and K. Matsumoto (2006). Raman investigation of strain in Si/SiGe heterostructures: Precise determination of the strain-shift coefficient of Si bands. *Journal of Applied Physics* **99**(5).

Nasdala, L., A. Kempe and R. Rolfes (2010). The Molecular Dynamic Finite Element Method (MDFEM). *CMC: Computers, Materials, & Continua* **19**: 57-104.

Ojeda, O. U. and T. Cagin (2010). Multiscale Modeling of Crystalline Energetic Materials. *CMC: Computers, Materials, & Continua* **16**: 127-174.

Pan, E. (2002). Mindlin's problem for an anisotropic piezoelectric half-space with general boundary conditions. *Proceedings of the Royal Society of London Series a-Mathematical Physical and Engineering Sciences* **458**(2017): 181-208.

Pan, E. and B. Yang (2001). Elastostatic fields in an anisotropic substrate due to a buried quantum dot. *Journal of Applied Physics* **90**(12): 6190-6196.

Pan, E. and B. Yang (2003). Elastic and piezoelectric fields in a substrate AlN due to a buried quantum. *Journal of Applied Physics* **93**(5): 2435-2439.

- Pan, E. and F. G. Yuan** (2000). Three-dimensional Green's functions in anisotropic bimetals. *International Journal of Solids and Structures* **37**(38): 5329-5351.
- Pham, H. H. and T. Tahir Cagin** (2010). Lattice Dynamics and Second and Third Order Elastic Constants of Iron at Elevated Pressures *CMC: Computers, Materials, & Continua* **16**: 175-194.
- Qteish, A. and R. Resta** (1988). Microscopic atomic-structure and stability of Si-Ge solid-solutions. *Physical Review B* **37**(3): 1308-1314.
- Qteish, A. and R. Resta** (1988). Thermodynamic properties of Si-Ge alloys. *Physical Review B* **37**(12): 6983-6990.
- Read, D. T. and V. K. Tewary** (2007). Multiscale model of near-spherical germanium quantum dots in silicon. *Nanotechnology* **18**(10): 105402.
- Roberts, M. M., L. J. Klein, D. E. Savage, K. A. Slinker, M. Friesen, G. Celler, M. A. Eriksson and M. G. Lagally** (2006). Elastically relaxed free-standing strained-silicon nanomembranes. *Nature Materials* **5**(5): 388-393.
- Saito, Y., M. Motohashi, N. Hayazawa, M. Iyoki and S. Kawata** (2006). Nanoscale characterization of strained silicon by tip-enhanced Raman spectroscopy in reflection mode. *Applied Physics Letters* **88**(14).
- Schaffler, F.** (1997). High-mobility Si and Ge structures. *Semiconductor Science and Technology* **12**(12): 1515-1549.
- Shen, S. and S. N. Atluri** (2004). Computational Nano-mechanics and Multi-scale Simulation *CMC: Computers, Materials, & Continua* **1**: 59-90.
- Stoney, G. G.** (1909). The tension of metallic films deposited by electrolysis. *Proceedings of the Royal Society of London Series A* **82**(553): 172-175.
- Tewary, V. K.** (1973). Green-Function Method for Lattice Statics. *Advances in Physics* **22**(6): 757- 810.
- Tewary, V. K.** (2004). Multiscale Green's-function method for modeling point defects and extended defects in anisotropic solids: Application to a vacancy and free surface in copper. *Physical Review B* **69**(9): 13.
- Tewary, V. K.** (2011). Phenomenological interatomic potentials for silicon, germanium and their binary alloy. *Physics Letters A* **375**: 3811-3816.
- Tewary, V. K. and D. T. Read** (2004). Integrated Green's function molecular dynamics method for multiscale modeling of nanostructures: Application to Au nanoisland in Cu. *CMES: Computer Modeling in Engineering & Sciences* **6**(4): 359-371.
- Tewary, V. K., R. H. Wagoner and J. P. Hirth** (1989). Elastic Green-Function for a Composite Solid with a Planar Interface. *Journal of Materials Research* **4**(1):

113-123.

Thomson, R., S. J. Zhou, A. E. Carlsson and V. K. Tewary (1992). Lattice Imperfections Studied by Use of Lattice Green-Functions. *Physical Review B* **46**(17): 10613-10622.

Torres, V. J. B., J. Coutinho, P. R. Briddon and M. Barroso (2008). Ab-initio vibrational properties of SiGe alloys. *Thin Solid Films* **517**(1): 395-397.

Vaudin, M. D., E. G. Kessler and D. M. Owen (2011). Precise silicon die curvature measurements using the NIST lattice comparator: comparisons with coherent gradient sensing interferometry. *Metrologia* **48**: 201-211.

Yakhno, V. G. (2011). Computation of Dyadic Green's Functions for Electrodynamics in Quasi-Static Approximation with Tensor Conductivity. *CMC: Computers, Materials, & Continua* **21**: 1-16.

Yang, B. and E. Pan (2002). Three-dimensional Green's functions in anisotropic trimaterials. *International Journal of Solids and Structures* **39**(8): 2235-2255.

Yang, B. and V. K. Tewary (2005). Green's function-based multiscale modeling of defects in a semi-infinite silicon substrate. *International Journal of Solids and Structures* **42**(16-17): 4722-4737.

Yang, B. and V. K. Tewary (2006). Efficient Green's function modeling of line and surface defects in multilayered anisotropic elastic and piezoelectric materials. *CMES: Computer Modeling in Engineering & Sciences* **15**(3): 165-177.

Yang, B. and V. K. Tewary (2007). Multiscale modeling of point defects in Si-Ge(001) quantum wells. *Physical Review B* **75**(14).

Yang, B. and V. K. Tewary (2008). Green's Function for Multilayers with Interfacial Membrane and Flexural Rigidities *CMC (Computers, Materials, & Continua)* **8**: 23-32.

Yu, M., C. S. Jayanthi, D. A. Drabold and S. Y. Wu (2001). Strain relaxation mechanisms and local structural changes in Si-Ge alloys. *Physical Review B* **64**: 1-8.

Zhu, R., E. Pan, P. W. Chung, X. Cai, K. M. Liew and A. Buldum (2006). Atomistic calculation of elastic moduli in strained silicon. *Semiconductor Science and Technology* **21**(7): 906-911.